HHS Public Access

Author manuscript

*Insect Biochem Mol Biol*. Author manuscript; available in PMC 2016 October 01.

Published in final edited form as:

*Insect Biochem Mol Biol*. 2015 October ; 65: 100–106. doi:10.1016/j.ibmb.2015.09.001.

# Carbonic anhydrase generates a pH gradient in *Bombyx mori* silk glands

**L.J. Domigan**[1,2,*], **M. Andersson**[3,*], **K.A. Alberti**[1], **M. Chesler**[4], **Q. Xu**[1], **J. Johansson**[3,5,6], **A. Rising**[3,5,¶], and **D.L. Kaplan**[1,¶]

[1]Department of Biomedical Engineering, Tufts University, Medford, Massachusetts, USA [2]School of Biological Sciences, The University of Auckland, Auckland, New Zealand [3]Department of Anatomy, Physiology and Biochemistry, Swedish University of Agricultural Sciences, Uppsala, Sweden [4]Departments of Neurosurgery, Physiology and Neuroscience, New York University School of Medicine, New York, New York, USA [5]Department of Neurobiology, Care Sciences and Society, Karolinska Institutet, Huddinge, Sweden [6]Institute of Mathematics and Natural Sciences, Tallinn University, Tallinn, Estonia

## Abstract

Silk is a protein of interest to both biological and industrial sciences. The silkworm, *Bombyx mori*, forms this protein into strong threads starting from soluble silk proteins using a number of biochemical and physical cues to allow the transition from liquid to fibrous silk. A pH gradient has been measured along the gland, but the methodology employed was not able to precisely determine the pH at specific regions of interest in the silk gland. Furthermore, the physiological mechanisms responsible for the generation of this pH gradient are unknown.

In this study, concentric ion selective microelectrodes were used to determine the luminal pH of *Bombyx mori* silk glands. A gradient from pH 8.2 to 7.2 was measured in the posterior silk gland, with a pH 7 throughout the middle silk gland, and a gradient from pH 6.8 to 6.2 in the beginning of the anterior silk gland where silk processing into fibers occurs. The small diameter of the most anterior region of the anterior silk gland prevented microelectrode access in this region. Using a histochemical method, the presence of active carbonic anhydrase was identified in the funnel and anterior silk gland of fifth instar larvae. The observed pH gradient collapsed upon addition of the carbonic anhydrase inhibitor methazolamide, confirming an essential role for this enzyme in pH regulation in the *Bombyx mori* silk gland. Plastic embedding of whole silk glands allowed clear visualization of the morphology, including the identification of four distinct epithelial cell types in

Corresponding authors: A. Rising, anna.rising@slu.se; D.L. Kaplan, david.kaplan@tufts.edu.

*,¶These authors made equal contributions

**Competing interests**

The authors have no competing interests to declare.

**Author contributions**

LD, MA, KA carried out experiments and data analysis. AR, JJ, DK assisted in experimental conception and design. MC, QX, AR, JJ, DK contributed reagents/materials/analysis tools. The manuscript was prepared by LD, MA with contribution from AR, JJ, DK.

the gland and allowed correlations between silk gland morphology and silk stages of assembly related to the pH gradient.

*Bombyx mori* silk glands have four different epithelial cell types, one of which produces carbonic anhydrase. Carbonic anhydrase is necessary for the mechanism that generates an intraluminal pH gradient, which likely regulates the assembly of silk proteins and then the formation of fibers from soluble silk proteins. These new insights into native silk formation may lead to a more efficient production of artificial or regenerated silkworm silk fibers.

## Graphical Abstract

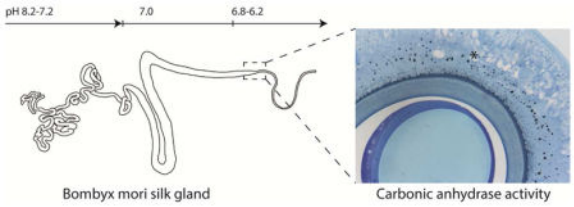


### Keywords

Fibroin; silk gland; ion-selective microelectrodes; morphology; carbonic anhydrase

## Background

The silkworm, *Bombyx mori*, produces proteins that are spun into insoluble fibers with exceptional properties. *B. mori* is a highly studied organism in life sciences due to its remarkably high level of protein synthesis during specific stages of its lifecycle. The unique properties of silk - strength and biocompatibility, mean it has attracted great interest as a biomaterial for tissue engineering, drug delivery and high technology interfaces (Altman et al., 2003; Omenetto and Kaplan, 2010). Aside from the biological interest, there remains a goal to mimic the natural process of silk spinning to generate fibers in a laboratory setting (Holland et al., 2012), leading to the ongoing investigation into the mechanisms involved *in vivo*.

*B. mori* produces silk proteins through unique biomolecular machinery contained in two silk glands. These glands are completely formed during embryonic development (Perdrix-Gillot, 1979). Silkworm larvae go through five larval molts and during this process the silk gland grows in size (to an organ over 15 cm long), although no further cell division takes place (Matsunami et al., 1999). Silk proteins (fibroin heavy (H) and light (L) chain, p25, and sericins) are produced in the silk gland during the larval life stage and spun into fibers for cocoon formation at the end of the $5^{th}$ larval instar.

Macroscopically, the silk glands of *B. mori* exist as two tubular structures which come together to form a spinneret, from which silk fibers are pulled via larval head movement (Magoshi et al., 1993). The silk gland is divided into three regions: the posterior silk gland (PSG), the middle silk gland (MSG), and the anterior silk gland (ASG) (Figure 1). The PSG is the site of fibroin synthesis, the MSG is responsible for the storage of fibroin as well as

the production of sericin proteins (Gamo et al., 1977; Kludkiewicz et al., 2009; Okamoto et al., 1982; Takasu et al., 2007), and the ASG is where the sol-gel transition of the silk takes place, with a viscous silk solution flowing to the spinneret (Akai, 1983). The spinneret consists of a silk press and a duct where the fiber exits through a pore on the worms lower lip (Asakura et al., 2007; Magoshi et al., 1993). The silk fiber consists of two fibroin protein filaments that consist mainly of heavy- and light-chain fibroins, in a one-to-one stoichiometry, linked by a disulfide bond. This filament is enveloped in a sericin coat that consists of several sericin proteins, produced by at least three genes (Gamo et al., 1977; Kludkiewicz et al., 2009; Okamoto et al., 1982; Takasu et al., 2007).

A number of factors are known to affect silk fiber formation in the silk glands of *B. mori*. These include changes in pH, ion concentrations ($Ca^{2+}$, $K^{+}$, $Cu^{2+}$), protein concentration, water content, and shear (Foo et al., 2006; Magoshi et al., 1993). It has previously been stated that the pH of the *B. mori* gland lumen ranges from approximately 6.9 in the PSG to 4.9 in the ASG (Magoshi et al., 1993; Miyake and Azuma, 2008a). However, the techniques used to measure pH in the gland utilized pH sensitive dyes. These dyes can approximate pH, yet they are unable to provide detailed pH values at specific points of interest in the gland. A detailed knowledge of the pH gradient is important since subtle changes in pH can dramatically influence the structure of the silk proteins (Foo et al., 2006; He et al., 2012; Terry et al., 2004), thus refined insight into the role of pH *in situ* would be critical to improving both the understanding of the silk transitions in the gland, as well as toward biomimetic systems designed to recapitulate the silk spinning process (Holland et al., 2007, 2012).

The presence of a pH gradient in the *B. mori* silk gland suggests an active acidification mechanism, which also correlates well with the pI of the silk fibroin (ExPASy pI/MW tool; Gattiker et al., 2003). Full details of this mechanism are unknown, although the presence of a vacuolar-type ATPase (V-ATPase) in the gland epithelium has been proposed to play a role in the generation of the pH gradient (Azuma and Ohta, 1998). A recent study found that the enzyme carbonic anhydrase (CA) is involved in establishing the pH gradient in silk glands of several spider species, including *Euprosthenops australis* and *Nephila clavipes* (Andersson et al., 2014). Remarkable similarities have been noticed in the mechanism of spinning and the structure of the silk gland from spiders and silkworms (Foo et al., 2006), despite the fact that the ability to spin silk in silkworms and spiders has arisen independently (Craig, 1997). These similarities warrant investigation into a role for carbonic anhydrase in pH regulation in *B. mori* silk glands.

In this study, the goal was to clarify the role and origin of pH gradients during silk processing. To address this goal, the use of plastic embedding enabled visualization of fifth instar silk gland morphology in greater detail than has previously been reported, revealing the presence of four different epithelial cell types in the *B. mori* silk gland. By using concentric ion selective microelectrodes (ISMs), precise determination of the pH in the different parts of the silk gland lumen was also achieved. Using a histochemical method that detects active CA (Ridderstråle, 1991), as well as inhibition experiments, we conclude that CA is necessary for the generation and maintenance of the pH gradient.

## Results

### Silk gland morphology

The silkworm (Figure 1A) progresses through five larval instars, accumulating large quantities of silk protein ready for cocoon spinning at the end of the fifth instar. The gland increases in size through the larval instars and in the fifth instar larvae, the S-shaped MSG (5 cm × 3 mm) occupies much of the abdomen of the worm, with the narrow and convoluted PSG (15 cm × 1.5 mm) in the proximal part of the worm and the tapering ASG (2 cm × 0.2 mm) leading up to the worm mouth (Figure 1B–C) where silk fibers are generated upon cocoon spinning.

### Four epithelial cell types in Bombyx mori silk gland

Using plastic embedded preparations of silk gland stained with hematoxylin and eosin (HE), and Azure blue, detailed cellular structures could be identified (Figure 2). Of particular interest was the identification of four different epithelial cell types that can be discerned through distinct staining with both HE and Azure blue. In the PSG the gland is lined with a single layer of tall (80 μm) columnar epithelial cells with elongated nuclei (Figure 2, A–B; cell type I). Here, the lumen of the gland contains a single homogenous material that stains light pink with HE and light blue with Azure blue (Figure 2, A–B). Moving into the middle region of the gland there is a change in cell morphology and two distinctly staining cell types (Figure 2, C–D; cell type II and III, image is at boundary of the two cell types). The gland becomes larger at this point and the columnar epithelial cells are wider, with distinct staining of granules between the two cell types (Figure 2, C–D). In the MSG a darker blue staining material in the lumen appears on Azure blue stained sections (Figure 2D). In the end of the MSG, a third layer in the lumen staining purple with HE and dark blue with Azure blue appears (Figure 2G and 4A). Towards the end of the MSG, where the gland narrows to form a funnel-like structure (Figure 2, E–F), there is a change in cell type (cell type IV) and the epithelial cells in this region exhibit a more compact, cuboidal morphology. At the funnel, there is also appearance of a cuticular intima (Figure 2, E–G). Cell type IV and the cuticular intima continue through the anterior gland (Figure 2G). All four cell types identified feature giant ramified nuclei. The locations of the four cell types are shown on the schematic of the gland in Figure 3.

### A broad gradient from pH 8 to 6 exists along the gland

Using concentric ISMs, the luminal pH of spinning fifth instar *B. mori* silk glands was measured at eleven different locations along the gland. A pH gradient from 8.2 – 6.2 was found from the PSG to the beginning of the ASG (Figure 3) with a surprisingly small difference between individuals.

### Carbonic anhydrase generates and maintains the pH gradient in the gland

Carbonic anhydrase activity was studied on historesin embedded sections from the posterior, middle, and anterior silk gland. The presence of a black precipitate is indicative of active CA in cell type IV, in the funnel and in the ASG (Figure 4; S1 (Supplementary Material)). The carbonic anhydrase activity seems to be localized to the apical cell membrane and to

intracellular granules (Figure 4, A–C). Treatment of glands with the CA inhibitor methazolamide resulted in inhibition of carbonic anhydrase activity (Figure S1 (Supplementary Material)), and caused the pH gradient to level out to approximately pH 7 (Figure 3).

## Discussion

Four different cell types were identified in the silk gland of *B. mori*. It is likely that cell type I in the PSG produces fibroin (Figure 2 A–B) while the two cell types (II and III) in the MSG may correspond to cells producing different sericin proteins (Figure 2 C–D). It is believed that the sericins secreted in the MSG does not mix with the fibroin and exist as a lubricating layer around the fibroin as the gland content is transported to the ASG (Magoshi et al., 1993). The presence of three differentially stained layers in the gland lumen (Figures 2G and 4A) support this notion. Cell type IV is responsible for producing carbonic anhydrase (Figure 4), discussed below. At the funnel, where cell type IV begins, a cuticular intima appears at the apical cell membrane (Figures 2E–G and 4A–B) and is present all along the ASG, similar to the cuticular intima that has been observed along the s-shaped duct in spider silk glands (Andersson et al., 2013). It has been proposed that the cuticle acts to resist unwanted deformation of the duct epithelium (Davies et al., 2013). The giant ramified nuclei present in all four cell types are characteristic of polyploidation, and have previously been identified in a number of lepidopteran species, including *B. mori* (Henderson and Locke, 1992; Ichimura et al., 1985). Through polyploidation, the genomic DNA content of the silk gland increases 200–400 thousand times during the larval lifespan via the process of endomitosis (Dhawan and Gopinathan, 2003; Perdrix-Gillot, 1979; Zhang et al., 2012a).

It has been stated that the pH of the gland lumen ranges from approximately 6.9 in the PSG to 4.9 in the ASG but it is unclear how this was measured (Magoshi et al., 1993). In another study, Miyake and Azuma focused on feeding (days 1–7) and spinning (days 8–11) fifth instar larvae. They approximated the pH of the gland lumen using the pH-sensitive dye phenol red (Miyake and Azuma, 2008b). Using this technique they observed a gradient from pH 7–8 in the PSG to pH 5–6 in the MSG in feeding larvae, and a neutral pH in the MSG of spinning larvae (the dye did not permeate the ASG in either case or the PSG in spinning larvae). Our detailed pH measurements using ISMs correlated well with the pH values in the MSG of spinning larvae (Miyake and Azuma, 2008b) but we find the pH of the proximal gland lumen to be higher than previously reported by Magoshi *et al*., with a pH gradient between 8.1 and 7.2 in the PSG, neutral pH throughout the MSG, a drop to pH 6.8 in the funnel, and a gradient from 6.5–6.2 in the beginning of the ASG (Figure 3). The presence of active carbonic anhydrase indicates that pH may continue to drop along the ASG but the small inner diameter (approximately 50 μm) in combination with the toughness of the cuticular intima of the anterior part of the ASG prevented measurements with the ISMs.

Of particular interest is the pH gradient in the ASG. The silk proteins undergo the silk I (random coil, helix and hydrated β-strand) to silk II (predominately β-sheet) transition in the ASG (Asakura et al., 1983, 1984). We have previously proposed a model for silk fiber assembly in which there is (i) self-assembly of micelle-like particles, that (ii) aggregate into

larger globules or gel in response to decreasing pH, and (iii) finally elongate and align under physical shear (Jin and Kaplan, 2003). Rheological data on dope extracted from the gland has shown that lowering and raising the pH with acetic acid (approximately pH 2) and ammonia (approximately pH 11) induced partially reversible gel formation at acidic pH (Terry et al., 2004). This has been attributed to the drop in pH promoting protonation of acidic side chains and allowing the formation hydrogen bonds that stabilize β-sheet and the gel state. This assumption is based upon the predicted pI of 4.2 for H-chain fibroin. The pH values measured in this study are all above 6 but could still allow protonation of carboxylate side-chains, as predicted pI values do not account for local perturbation of side-chain pKa values, which can for example be caused by clustering of charged residues, such as what was observed for the spider silk N-terminal domain (Askarieh et al., 2010; Kronqvist et al., 2014). The pH values measured in this study would allow for the silk dope to exist as a weak gel in the funnel and ASG that can still flow to the spinneret.

On the molecular level, structural data have shown that the fibroin N-terminal domain, thought to be essential in mediating silk fiber assembly, undergoes a pH-induced conformational transition from random coil to β-sheet between pH 7.0 and 6.0 thereby likely triggering silk assembly (He et al., 2012). Dynamic light scattering on fibroin N-terminal domain showed that oligomerization also takes place in a pH responsive manner between pH 7.0 and 6.0 (He et al., 2012). From the funnel to the beginning of the ASG we show a pH gradient from approximately pH 7 to pH 6, which again supports the funnel/ASG as the primary region where the structural transformation of fibroin N-terminal domain takes place.

Cell type IV, which is present all along the ASG, produces carbonic anhydrase (Figure 4). Thus, the region in which there is CA activity starts where there is no longer production of fibroins. CA activity observed in the major ampullate gland of the spider, *E. australis* was also seen to commence at the site where the silk proteins, spidroins, cease to be produced (Andersson et al., 2014). Histochemical methods have proved useful in localizing enzymes that may be important to the silk spinning process (Azuma and Ohta, 1998; Azuma et al., 2012; Miyake and Azuma, 2008a). As mentioned previously, a $H^+$-translocating vacuolar-type ATPase (V-ATPase) is located at the apical plasma membrane of the ASG, as well as in the posterior part of the MSG (Azuma et al., 2001), with a role in pumping $H^+$ into the lumen of the gland (Azuma and Ohta, 1998). CA activity in the funnel and ASG of spinning larvae may complement these proton pumps, in lowering the pH of the gland.

As mentioned previously, the abilities to spin silk in silkworms and spiders have arisen independently (Craig, 1997). Despite this difference in origin, there are remarkable similarities in the spinning mechanisms in silkworm and spider silk glands. The spider silk gland also consists of a single tall epithelial cell layer (Andersson et al., 2013; Kovoor, 1987). The tail in spider silk glands, which corresponds to the PSG of silkworms, has luminal pH above 7.5 (Andersson et al., 2014; Dicko et al., 2004), and its main function is protein production (Andersson et al., 2013). The posterior part of the sac, corresponding to the MSG in silkworm, produces protein and holds a neutral pH, while the duct, corresponding to the ASG, produces carbonic anhydrase and has a steep pH gradient which likely reaches below pH 5.7 (Andersson et al., 2014). Furthermore, it has been shown that in this pH interval, the fibroin N-terminal domain undergoes a conformational change (He et

al., 2012), which likewise has been shown for the spider silk protein N- (Askarieh et al., 2010; Gaines et al., 2010; Kronqvist et al., 2014, Otikovs et al., 2015) and C-terminal domain (Andersson et al., 2014, Gauthier et al., 2014). These similarities between the two species indicate that the mechanism of spinning may be more universal than previously anticipated.

The efficient and elegant way that *B. mori* produces strong silk fibers, all under physiological conditions at ambient temperature and without the need for toxic solvents and high pressure, has led to an interest in biomimetic processing of silk in a laboratory setting (Holland et al., 2012). Production of non-native silk fibers involves attention to both the production of the regenerated silk solution and the mode of spinning (Holland et al., 2007). Wet spinning, electrospinning, and dry spinning have all attempted to mimic silkworm spinning of regenerated silk solutions, however, most of these approaches oversimplify this complex process and as a result the silk fibers produced often lack desirable properties (Fu et al., 2009; Kinahan et al., 2011; Wei et al., 2011; Zhang et al., 2012b). A recent study by Zhang *et al.* produced silk fibers via wet spinning with mechanical properties that matched those of the native silk fiber. This can be attributed to their approach, with regenerated fibroin produced under milder conditions - maintaining some of the hierarchical structure of native silk fibers, and the use of water as a coagulant (Zhang et al., 2015). The elucidation of the underlying mechanisms behind the hierarchical assembly and structural transitions observed in silk fiber formation is important information to guide biomimetic silk processing.

## Conclusions

Four different epithelial cell types exist in the silk gland of fifth instar spinning *B. mori* larvae, one of which produces active carbonic anhydrase. The carbonic anhydrase generates and maintains a pH gradient ranging from pH 8.2 to 7.2 in the PSG, 7.2-7 in the MSG and 6.8 to 6.2 in the ASG. The data presented will likely be of importance for the development of biomimetic artificial silk fibers.

## Materials and Methods

### Animals

A *B. mori* colony was established with animals obtained from Coastal Silkworms (Florida, USA). Silkworms were raised at room temperature (25° ± 1°C) on fresh mulberry leaves. For this study the life-stage of interest was $5^{th}$ instar larvae at full maturation that have commenced spinning. At this stage the larvae stop eating and bodies become yellowish. The larvae then soon start spinning to make a cocoon.

### Tissue processing and Histology

Silkworms were anesthetized on ice and the silk gland removed via an incision along the ventral side of the larvae. Dissections were carried out in physiological saline (pH 7.4). The gland was removed and sectioned according to Figure 1, in order to obtain the posterior, middle, and anterior regions of the gland. Tissues were fixed in 2.5 % (v/v) glutaraldehyde in phosphate buffered saline (PBS) (pH 7.2) for 24 hours at 4°C and subsequently rinsed

with PBS (pH 7.2). After fixation, tissues were dehydrated using increasing concentrations of ethanol, infiltrated and embedded in water-soluble glycol methacrylate (Leica Historesin embedding kit). Historesin embedded silk glands were sectioned at 2 μm using a microtome (Leica RM 2165) and stained with HE or Azure blue. Imaging was performed on a Nikon Microphot-FXA microscope and photos were taken with a Nikon Digitalsight DS-SM camera. Cryoembedding and sectioning was also carried out with glutaraldehyde fixed glands rinsed three times in PBS and then sucrose infused (30% sucrose solution, incubated at 4°C for 24 hours). The tissue was embedded in O.C.T. Compound (Tissue-Tek®) and sectioned at 10 μm using a cryomicrotome (Leica CM 1950).

### Histochemical localization of carbonic anhydrase activity

Historesin embedded silk glands from spinning fifth instar larvae were sectioned at 2 μm using a microtome (Leica RM 2165) and stained for CA activity using a histochemical method (Ridderstråle, 1991). This method involves the incubation of sections in a solution ($NaHCO_3/CoSO_4/H_2SO_4/KH_2PO_4$) that results in the formation of a cobalt-phosphate-carbonate complex, which is then converted into a black cobalt-sulphide precipitate at sites of CA activity. Some sections were counterstained with Azure blue. For control of unspecific staining, the CA inhibitor acetazolamide was included in the incubation solution.

### pH measurements in Bombyx mori silk glands

Concentric ISMs were used to measure the concentration of hydrogen ions in various regions of the silk glands from spinning fifth instar larvae. These were prepared as per (Fedirko et al., 2006), and calibrated using pH 6.87 and pH 7.42 buffers. Whole silk glands were dissected as previously described, differing only in that the dissection was carried out in a modified Spider Ringer (Shartau et al 1983) solution (2 mM $MgCl_2$, 2 mM $CaCl_2$, 3 mM KCl, and 10 mM glucose) buffered with 26 mM bicarbonate and 5% $CO_2$, giving a pH of 7.4. Silk glands were mounted in a Sylgard® submersion style incubation chamber and superfused with Ringer solution at room temperature. Ion-selective microelectrode measurements were performed in eleven regions of the gland, as indicated in Figure 3 and a triplicate measurement was performed at each location, in every gland. The difference in potential between the Ringer and inside of the silkworm gland was recorded on a chart recorder (Zipp and Konnen) and translated into change in concentration of hydrogen ions using the Nernst equation.

To study the influence of CA activity on the pH gradient, some glands were treated with a membrane-permeable carbonic anhydrase inhibitor, methazolamide (M4156 Fluka) for 30 minutes in 0.1 mM methazolamide (M4156, Fluka) before pH measurements. This was done by incubation of the excised silk glands in Ringer solution containing methazolamide. The effect of incubation time on the pH gradient was accounted for by incubation of silk glands for 30 min in Ringers solution only – with no effect on the pH gradient seen.

## Supplementary Material

Refer to Web version on PubMed Central for supplementary material.

## Acknowledgments

We thank the NIH (P41 EB002520, the NSF (IGERT) and the AFOSR for support for this work. We also thank the SLU fund for internationalisation of doctoral studies.

## List of abbreviations

| | |
|---|---|
| **PSG** | Posterior silk gland |
| **MSG** | Middle silk gland |
| **ASG** | Anterior silk gland |
| **V-ATPase** | Vacuolar ATPase |
| **CA** | Carbonic anhydrase |
| **ISMs** | Ion-selective microelectrodes |
| **HE** | Hematoxylin and eosin |
| **PBS** | Phosphate buffered saline |

## References

Akai H. The structure and ultrastructure of the silk gland. Experientia. 1983; 39:443–449.

Altman GH, Diaz F, Jakuba C, Calabro T, Horan RL, Chen J, Lu H, Richmond J, Kaplan DL. Silk-based biomaterials. Biomaterials. 2003; 24:401–416. [PubMed: 12423595]

Andersson M, Holm L, Ridderstrale Y, Johansson J, Rising A. Morphology and Composition of the Spider Major Ampullate Gland and Dragline Silk. Biomacromolecules. 2013; 14:2945–2952. [PubMed: 23837699]

Andersson M, Chen G, Otikovs M, Landreh M, Nordling K, Kronqvist N, Westermark P, Jornvall H, Knight S, Ridderstrale Y, et al. Carbonic Anhydrase Generates CO2 and H+ That Drive Spider Silk Formation Via Opposite Effects on the Terminal Domains. Plos Biol. 2014; 12:e1001921. [PubMed: 25093327]

Asakura T, Suzuki H, Watanabe Y. Conformational characterization of silk fibroin in intact Bombyx mori and Pilosamia cynthia ricini silkworms by carbon-13 NMR spectroscopy. Macromolecules. 1983; 16:1024–1026.

Asakura T, Watanabe Y, Uchida A, Minagawa H. NMR of silk fibroin. Carbon-13 NMR study of the chain dynamics and solution structure of Bombyx mori silk fibroin. Macromolecules. 1984; 17:1075–1081.

Asakura T, Umemura K, Nakazawa Y, Hirose H, Higham J, Knight D. Some Observations on the Structure and Function of the Spinning Apparatus in the Silkworm Bombyx mori. Biomacromolecules. 2007; 8:175–181. [PubMed: 17206804]

Askarieh G, Hedhammar M, Nordling K, Saenz A, Casals C, Rising A, Johansson J, Knight SD. Self-assembly of spider silk proteins is controlled by a pH-sensitive relay. Nature. 2010; 465:236–238. [PubMed: 20463740]

Azuma M, Ohta Y. Changes in H+-translocating vacuolar-type ATPase in the anterior silk gland cell of Bombyx mori during metamorphosis. J Exp Biol. 1998; 201:479–486. [PubMed: 9438824]

Azuma M, Miyamoto Y, An Z. The Distribution of H+-Translocating Vacuolar-Type ATPase in the Middle Silk Gland Cell of Bombyx mori. J Insect Biotechnol Sericology. 2001; 70:25–32.

Azuma M, Nagae T, Maruyama M, Kataoka N, Miyake S. Two water-specific aquaporins at the apical and basal plasma membranes of insect epithelia: Molecular basis for water recycling through the cryptonephric rectal complex of lepidopteran larvae. J Insect Physiol. 2012; 58:523–533. [PubMed: 22285686]

Craig CL. Evolution of Arthropod Silks. Annu Rev Entomol. 1997; 42:231–267. [PubMed: 15012314]

Davies GJG, Knight DP, Vollrath F. Chitin in the Silk Gland Ducts of the Spider Nephila edulis and the Silkworm Bombyx mori. Plos One. 2013; 8:e73225. [PubMed: 24015298]

Dhawan S, Gopinathan KP. Cell cycle events during the development of the silk glands in the mulberry silkworm Bombyx mori. Dev Genes Evol. 2003; 213:435–444. [PubMed: 12883881]

Dicko C, Vollrath F, Kenney JM. Spider Silk Protein Refolding Is Controlled by Changing pH. Biomacromolecules. 2004; 5:704–710. [PubMed: 15132650]

Fedirko N, Svichar N, Chesler M. Fabrication and use of high-speed, concentric H+- and Ca2+-selective microelectrodes suitable for in vitro extracellular recording. J Neurophysiol. 2006; 96:919–924. [PubMed: 16672303]

Foo CWP, Bini E, Hensman J, Knight DP, Lewis RV, Kaplan DL. Role of pH and charge on silk protein assembly in insects and spiders. Appl Phys -Mater Sci Process. 2006; 82:223–233.

Fu C, Shao Z, Fritz V. Animal silks: their structures, properties and artificial production. Chem Commun. 2009:6515–6529.

Gaines WA, Sehorn MG, Marcotte WR. Spidroin N-terminal Domain Promotes a pH-dependent Association of Silk Proteins during Self-assembly. J Biol Chem. 2010; 285:40745–40753. [PubMed: 20959449]

Gamo T, Inokuchi T, Laufer H. Polypeptides of fibroin and sericin secreted from the different sections of the silk gland in Bombyx mori. Insect Biochem. 1977; 7:285–295.

Gattiker A, Hoogland C, Iranyi I, Appel RD, Bairoch A. ExPASy: the proteomics server for in-depth protein knowledge and analysis. Nucleic Acids Res. 2003; 31:3784–3788. [PubMed: 12824418]

Gauthier M, Leclerc J, Lefèvre T, Gagné SM, Auger M. Effect of pH on the structure of the recombinant C-terminal domain of Nephila clavipes dragline silk protein. Biomacromolecules. 2014; 15(12):4447–4454. [PubMed: 25337802]

He YX, Zhang NN, Li WF, Jia N, Chen BY, Zhou K, Zhang J, Chen Y, Zhou CZ. N-Terminal Domain of Bombyx mori Fibroin Mediates the Assembly of Silk in Response to pH Decrease. J Mol Biol. 2012; 418:197–207. [PubMed: 22387468]

Henderson S, Locke M. A Shell of F-Actin Surrounds the Branched Nuclei of Silk Gland-Cells. Cell Motil Cytoskeleton. 1992; 23:169–187.

Holland C, Terry AE, Porter D, Vollrath F. Natural and unnatural silks. Polymer. 2007; 48:3388–3392.

Holland C, Vollrath F, Ryan AJ, Mykhaylyk OO. Silk and Synthetic Polymers: Reconciling 100 Degrees of Separation. Adv Mater. 2012; 24:105–109. [PubMed: 22109705]

Ichimura S, Mita K, Zama M, Numata M. Isolation of the Giant Ramified Nuclei of the Posterior Silk Glands of Bombyx-Mori. Insect Biochem. 1985; 15:277–283.

Jin HJ, Kaplan DL. Mechanism of silk processing in insects and spiders. Nature. 2003; 424:1057–1061. [PubMed: 12944968]

Kinahan ME, Filippidi E, Köster S, Hu X, Evans HM, Pfohl T, Kaplan DL, Wong J. Tunable Silk: Using Microfluidics to Fabricate Silk Fibers with Controllable Properties. Biomacromolecules. 2011; 12:1504–1511. [PubMed: 21438624]

Kludkiewicz B, Takasu Y, Fedic R, Tamura T, Sehnal F, Zurovec M. Structure and expression of the silk adhesive protein ser2 in Bombyx mori. Insect Biochem Mol Biol. 2009; 39:938–946. [PubMed: 19995605]

Kovoor, J. Comparative Structure and Histochemistry of Silk-Producing Organs in Arachnids. In: Nentwig, W., editor. Ecophysiology of Spiders. Springer; Berlin Heidelberg: 1987. p. 160-186.

Kronqvist N, Otikovs M, Chmyrov V, Chen G, Andersson M, Nordling K, Landreh M, Sarr M, Jornvall H, Wennmalm S, et al. Sequential pH-driven dimerization and stabilization of the N-terminal domain enables rapid spider silk formation. Nat Commun. 2014; 5:3254. [PubMed: 24510122]

Magoshi, J.; Magoshi, Y.; Nakamura, S. Silk Polymers. American Chemical Society; 1993. Mechanism of Fiber Formation of Silkworm; p. 292-310.

Matsunami K, Kokubo H, Ohno K, Xu PX, Ueno K, Suzuki Y. Embryonic silk gland development in Bombyx: molecular cloning and expression of the Bombyx trachealess gene. Dev Genes Evol. 1999; 209:507–514. [PubMed: 10502107]

Miyake S, Azuma M. Developmental expression and the physiological role of aquaporin in the silk gland of Bombyx mori. J Insect Biotechnol Sericology. 2008; 77:87–93.

Miyake S, Azuma M. Acidification of the Silk Gland Lumen in Bombyx mori and Samia cynthia ricini and Localization of H+-Translocating Vacuolar-Type ATPase. J Insect Biotechnol Sericology. 2008; 77:1_9–1_16.

Omenetto FG, Kaplan DL. New Opportunities for an Ancient Material. Science. 2010; 329:528–531. [PubMed: 20671180]

Okamoto H, Ishikawa E, Suzuki Y. Structural analysis of sericin genes. J Biol Chem. 1982; 257:15192–15199. [PubMed: 6294094]

Otikovs M, Chen G, Nordling K, Landreh M, Meng Q, Jörnvall H, Kronqvist N, Rising A, Johansson J, Jaudzems K. Diversified structural basis of a conserved molecular mechanism for pH dependent dimerization in spider silk N-terminal domains. ChemBioChem. 201510.1002/cbic.201500263

Perdrix-Gillot S. DNA synthesis and endomitoses in the giant nuclci of the silkgland of Bombyx mori. Biochimie. 1979; 61:171–204. [PubMed: 465570]

Ridderstråle, Y. Localization of Carbonic Anhydrase by Chemical Reactions. In: Dodgson, S.; Tashian, R.; Gros, G.; Carter, N., editors. The Carbonic Anhydrases. Springer; US: 1997. p. 133-144.

Takasu Y, Yamada H, Tamura T, Sezutsua H, Mita K, Tsubouchi K. Identification and characterization of a novel sericin gene expressed in the anterior middle silk gland of the silkworm Bombyx mori. Insect Biochem Mol Biol. 2007; 37:1234–1240. [PubMed: 17916509]

Terry AE, Knight DP, Porter D, Vollrath F. pH induced changes in the rheology of silk fibroin solution from the middle division of Bombyx mori silkworm. Biomacromolecules. 2004; 5:768–772. [PubMed: 15132659]

Wei W, Zhang Y, Zhao Y, Luo J, Shao H, Hu X. Bio-inspired capillary dry spinning of regenerated silk fibroin aqueous solution. Mater Sci Eng C. 2011; 31:1602–1608.

Zhang CD, Li FF, Chen XY, Huang MH, Zhang J, Cui H, Pan MH, Lu C. DNA replication events during larval silk gland development in the silkworm, Bombyx mori. J Insect Physiol. 2012; 58:974–978. [PubMed: 22609363]

Zhang F, Zuo B, Fan Z, Xie Z, Lu Q, Zhang X, Kaplan DL. Mechanisms and Control of Silk-Based Electrospinning. Biomacromolecules. 2012; 13:798–804. [PubMed: 22300335]

Zhang F, Lu Q, Yue X, Zuo B, Qin M, Li F, Kaplan DL, Zhang X. Regeneration of high-quality silk fibroin fiber by wet spinning from CaCl2–formic acid solvent. Acta Biomater. 2015; 12:139–145. [PubMed: 25281787]

## Highlights

- Concentric ion selective microelectrodes were used to accurately determine the intraluminal pH of the *Bombyx mori* silk gland.
- A gradient from pH 8.2 (posterior) down to pH 6.2 (anterior) was recorded.
- Four distinct epithelial cell types were identified, one of which produces carbonic anhydrase.
- The pH gradient was found to collapse on inhibition of carbonic anhydrase, confirming an essential role for this enzyme in silk fiber production.

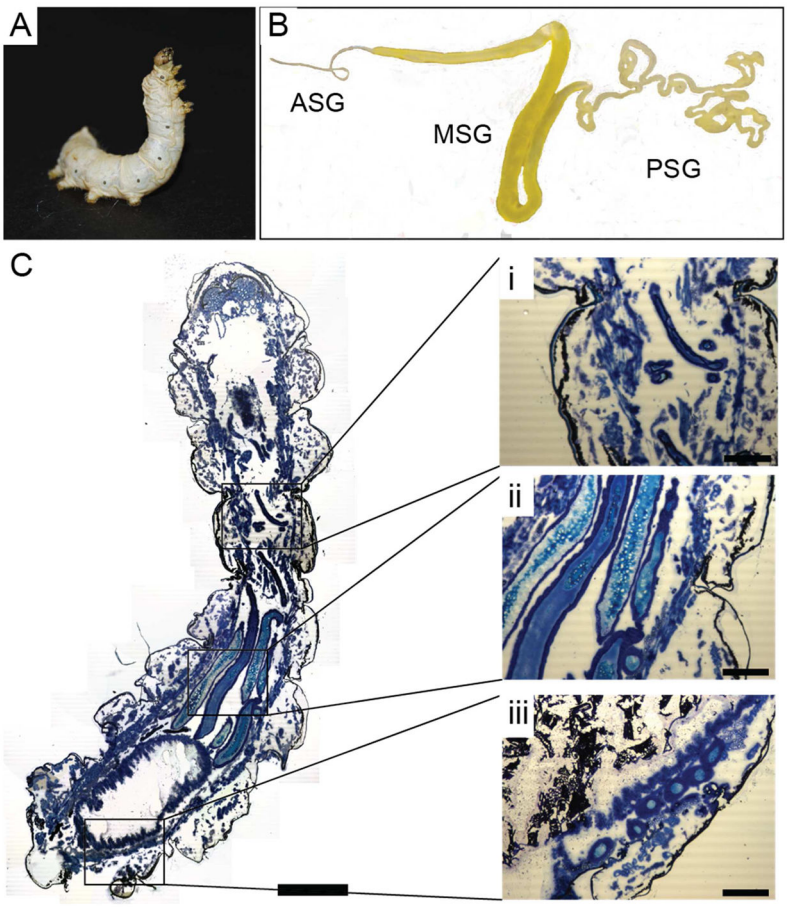


**Figure 1. Macroscopic structure of gland**

(A) *Bombyx mori* 5$^{th}$ instar larvae in the spinning stage. (B) Silk gland dissected from 5$^{th}$ instar larvae indicating the posterior silk gland (PSG), middle silk gland (MSG), and anterior silk gland (ASG). (C) Longitudinal cryosections of a whole 5$^{th}$ instar larvae stained with Toluene blue, with insets showing the (i) ASG, (ii) MSG and (iii) PSG. Scale bars 0.5 cm (C) and 200 μm (i, ii, iii).

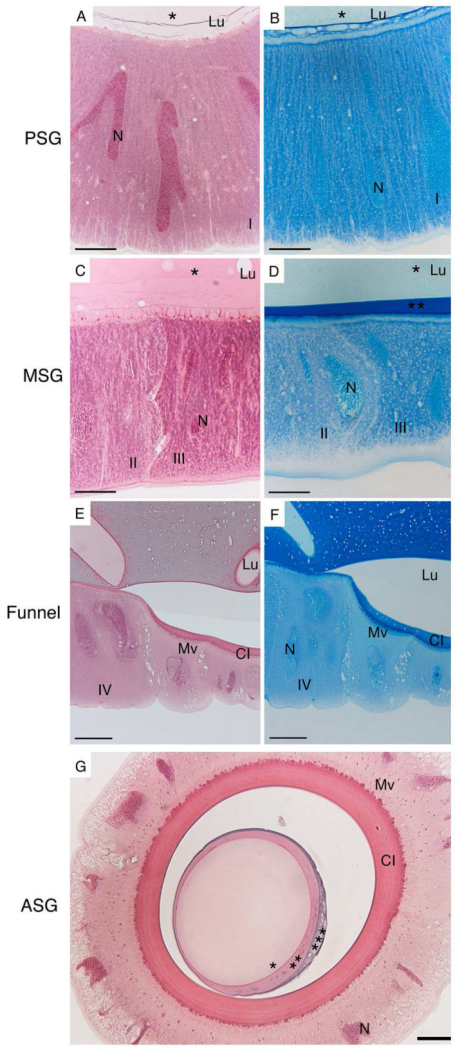


**Figure 2. Histology of the silk gland**

HE and Azure blue staining of the silk gland of 5$^{th}$ instar *B. mori* showing the presence of at least four (labelled I – IV) epithelial cell types. Scale bars are 20 μm (A–D, G) and 50 μm (E–F). PSG: posterior silk gland, MSG: middle silk gland, ASG: anterior silk gland, Lu: lumen, N: nucleus, Mv: microvilli, CI: cuticular intima, * indicates layer I, ** indicates layer II, *** indicates layer III.

| | PSG | | MSG | | | | Funnel ASG | | | | |
|---|---|---|---|---|---|---|---|---|---|---|---|
| Location | 1 | 2 | 3 | 4 | 5 | 6 | 7 | 8 | 9 | 10 | 11 |
| pH ± SD | 8.2 ± 0.1 | 7.7 ± 0.2 | 7.2 ± 0.1 | 7.2 ± 0.3 | 7.1 ± 0.2 | 7.1 ± 0.2 | 7.0 ± 0.1 | 6.8 ± 0.1 | 6.5 ± 0.1 | 6.5 ± 0.1 | 6.2 |
| n | 5 | 10 | 5 | 6 | 12 | 10 | 9 | 11 | 7 | 4 | 1 |
| + MTZ pH ± SD | | 7.2 ± 0.3 | | | | | | | 7.1 ± 0.1 | | |
| n | | 6 | | | | | | | 5 | | |

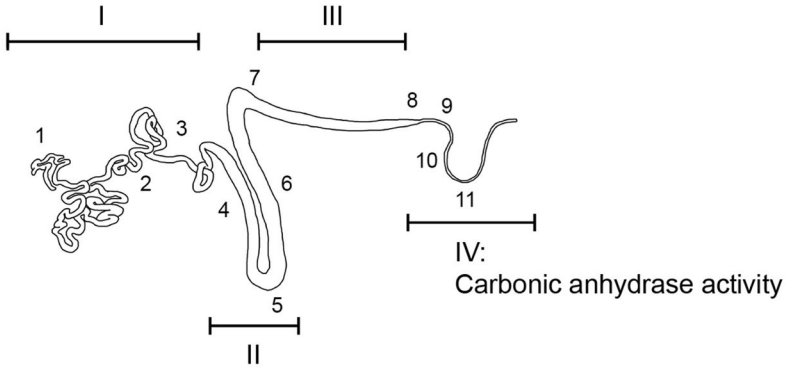


**Figure 3. pH of *Bombyx mori* silk gland**

Intraluminal pH (± SD) of the silk gland recorded at 11 locations (see schematic below table) in n number of glands. pH measurements were performed on dissected glands in an insect Ringer solution using ion-selective microelectrodes. pH measurements were also carried out following incubation of dissected glands in methazolamide (+MTZ). I – IV: refer to regions where different epithelial cell types were identified. Carbonic anhydrase activity was found in cell type IV and is identified on the gland schematic.

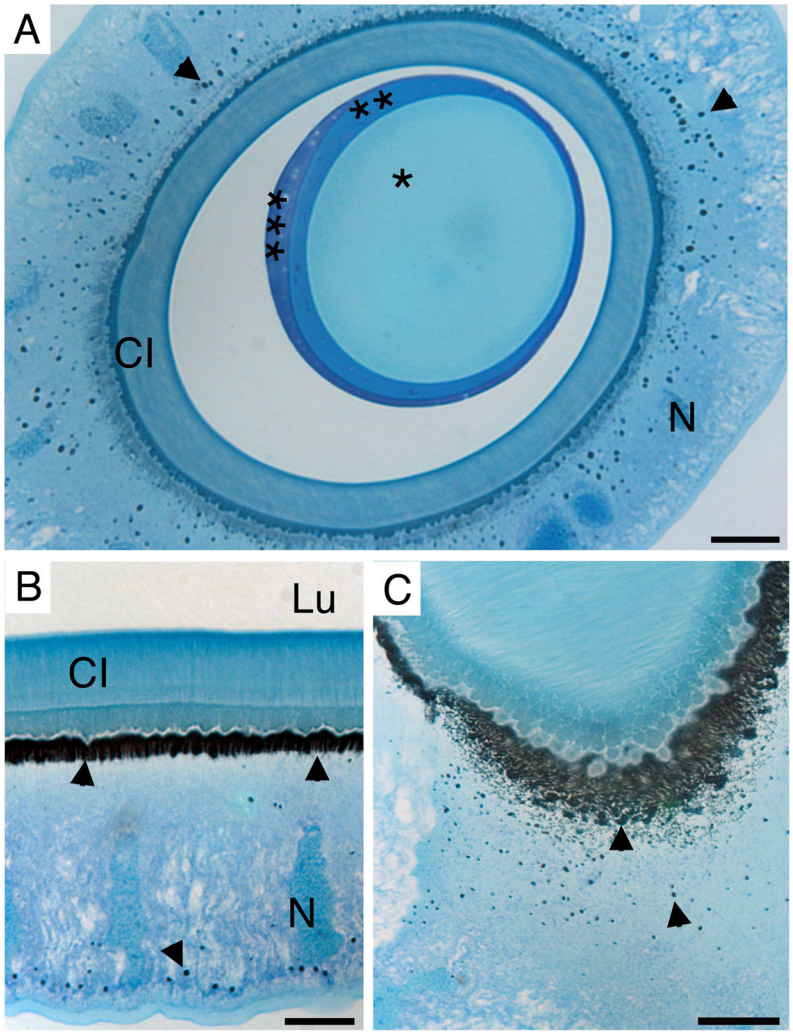


**Figure 4. Carbonic anhydrase activity in the anterior silk gland**

Cross-section (A) and longitundinal section (B and C) of the ASG stained for carbonic anhydrase activity (black precipitate, arrow heads) counterstained with Azure blue. Three distinct layers (*, **, and *** respectively) of the forming fiber in the lumen are visible. Scale bars are 20 μm (A and C) and 10 μm (B). CI: cuticular intima, N: nucleus, Lu: lumen.